Imaging of morphological changes and phase segregation in doped polymeric semiconductors

Felix Deschler[a,±], Daniel Riedel[a‡], Andras Deák[b], Bernhard Ecker[c÷], Elizabeth von Hauff[c] and Enrico Da Como[*,d]

[a]Photonics and Optoelectronics Group, Department of Physics and CeNS, Ludwig-Maximilians-Universität München, Munich 80799 Germany

[b]Research Institute of Technical Physics and Materials Science, Hungarian Academy of Sciences, Budapest, Hungary

[c]Organic Photovoltaics and Electronics Group, Institute of Physics, Albert-Ludwig-Universität Freiburg and Fraunhofer Institute for Solar Energy Systems (ISE) Freiburg, Germany

[d]Department of Physics, University of Bath, Claverton Down, Bath BA2 7AY, United Kingdom

ABSTRACT

The electrical conductivity and morphological characteristics of two conjugated polymers, P3HT and PCPDTBT, p-doped with the strong electron acceptor tetrafluoro-tetracyanoquinodimethane (F4-TCNQ) are studied as a function of dopant concentration. By combining scanning and transmission electron microscopy, SEM and TEM, with electrical characterisation we observe a correlation between the saturation in electrical conductivity and the formation of dopant rich clusters. We demonstrate that SEM is a useful technique to observe imaging contrast for locating doped regions in thin polymer films, while in parallel monitoring the surface morphology. The results are relevant for the understanding of structure property relationships in doped conjugated polymers.

*** Corresponding author: Tel. +441225-384368, Fax +441225-386110, Email edc25@bath.ac.uk**

1. INTRODUCTION

A prerequisite for the success of organic electronics in the current information-technology and renewable energy markets is performance and reliability. Recent scientific efforts towards this milestone focus on the use of dopant molecules to improve the electrical transport characteristics of light emitting diodes and solar cells [1-4]. Doping has been also demonstrated to be critical for tuning the carrier injection properties at metal-semiconductor interfaces, potentially leading to full control over device parameters [5-7]. Spatially controlled positioning of dopants can be used to tune injection [6, 8], improve carrier drift/diffusion in transport layers [9-11] and also charge separation at heterojunctions [12].

In organic devices based on small molecules, control of dopant positioning can be achieved by sequential evaporation of individual materials to form layered stacks [1]. In contrast, the controlled positioning of dopants in solution processable organic semiconductors, such as conjugated polymers, remains a challenge. Particularly for low mobility solution deposited materials, there is substantial interest in tuning electronic processes by doping[13, 14]. The physical origin of doping, i.e. the interactions between the organic semiconductor and dopant molecule, has recently seen renewed interest [15] [16, 17]. Systematic studies of carrier transport properties as a function of the dopant/semiconductor weight ratio often demonstrate saturation in the t key parameters (mobility and conductivity) above a certain threshold [13, 18]. However, there are few detailed investigations on the correlation between morphology and the efficacy of doping [19, 20].

While the influence of dopants on the electrical parameters of organic semiconductors has been addressed, one crucial question that has been poorly addressed is the morphology of the doped semiconductors, i.e. the distribution of dopants in the film but more critically, the role of (charged) dopant molecules in changing the organic semiconductor *morphology*. This latter aspect is expected to be highly relevant considering the widely reported and discussed effects of meso-morphology on the optical and electrical characteristics of organic semiconductors [21-23]. In this respect, experiments performed by Kahn and co-workers on imaging single dopants by STM [15] are extremely valuable, but limited to very thin films exhibiting the high crystallinity required for this technique. Very recently, Donhauser et al.[24] have reported the imaging of *inorganic dopant clusters* in vacuum sublimed small molecule films by transmission electron microscopy, suggesting the utility of electron microscopy to study doped organic semiconductor films. It is apparent that experimental strategies are

required which allow for the visualisation of dopant distributions and resulting mesoscopic morphology of doped polymeric films.

Here, we present a study on the morphology of two widely-studied conjugated polymers: Poly[2,1,3-benzothiadiazole-4,7-diyl[4,4-bis(2-ethylhexyl)-4H-cyclopenta[2,1-b:3,4-b']dithiophene-2,6-diyl]] (PCPDTBT) and poly(3-hexylthiophene) (P3HT) doped at different concentrations with the organic molecule 2,3,5,6-tetrafluoro-7,7,8,8-tetracyanoquinodimethane (F4-TCNQ). The polymeric materials are known to be model systems for solar cells and field effect transistors, respectively. Our material choice was also motivated by the idea of comparing polymers with intrinsically different electronic structures; PCPDTBT is a prototype donor-acceptor *copolymer* with an intrachain charge transfer character [25, 26], while P3HT is a prototypical conjugated *homopolymer* based on thiophene repeat units. Since both PCPDTBT and P3HT are well-known hole transporting materials we p-doped them with the strong electron acceptor F4-TCNQ. To the best of our knowledge we are not aware of studies on the morphology of doped conjugated *copolymers* such as PCPDTBT. We show that low voltage (<1kV) scanning electron microscopy (SEM) can in parallel monitor the film surface morphology and the dopant distribution with nanometer spatial resolution in the film plane. We comment on the origin of this useful contrast by comparing the surface morphological information from SEM with results from atomic force microscopy (AFM). In addition, we cross correlate the doping induced contrast in SEM with photoluminescence (PL) confocal imaging which is sensitive to doping because of localised PL quenching. We report on morphology changes in the polymer films and clustering of dopants at two different critical concentrations for the two polymers. Interestingly, the critical concentrations are directly correlated to the saturation in conductivity of the films investigated by electrical measurements. The results highlight SEM as a tool to investigate the morphology of doped polymeric semiconductors and suggest a correlation between morphology and saturation in conductivity for doped conjugated polymers.

2. MATERIALS AND METHODS

Materials and electrical characterization: P3HT (regioregularity > 95%, M_w ~ 30000 g/mol) was purchased from Sigma-Aldrich and used as received. PCPDTBT (M_w ~ 20000 g/mol) was purchased from 1-material and used as received. Chlorobenzene from Sigma Aldrich (HPLC, spectroscopic grade, anhydrous) was used as solvent to prepare solutions which were stirred for 24 hours at room temperature before deposition also at room temperature (20 °C). All concentration ratios are given in weight/weight% (w/w%). Samples for SEM/AFM were

prepared with a home made doctor blade on silicon wafer with a thin layer of native oxide. Samples for photoluminescence mapping were prepared by coating on thin microscope slides from the same solutions used for the SEM/AFM samples. For conductivity experiments the films were prepared inside a nitrogen filled glove-box on pre-structured Indium-Tin-oxide (ITO) coated glass substrates with an interdigitated channel: length of 75 cm, width of 70 μm and ITO thickness of 150 nm. The geometry constant was 6.22 cm^{-1}. Film thickness, 100 ±10 nm for all samples, was measured with a profilometer. The resistance was obtained from 4-probe measurements performed with a potentiostat/impedance module at Vac = 20 mV in the frequency range from 100 kHz - 1Hz in the dark and in a nitrogen atmosphere.

Electron microscopy: SEM Images were recorded with a Zeiss Ultra-Plus operating at 750 V accelerating voltage. Working distance was kept at 3.5 mm to ensure high collection efficiency of secondary electrons aided by the electrostatic lens and allowing efficient detection secondary electrons (SE2) simultaneously. Good electric contact with the sample stage was ensured for all samples to avoid any undesired charge build-up in the substrate. The microscope stage was not biased for any of the experiments. Transmission electron microscopy (TEM) images were obtained with a JEOL microscope operated at 100 kV. Image analysis was carried out using the software ImageJ. For the analysis, images taken at 25.000X magnification were used in all cases, with ca. 12 nm/pixel resolution. See supporting material for further details.

Confocal laser scanning photoluminescence microscopy: Photoluminescence maps were taken with an Olympus IX81 FVSF-2 with an UPLANFL N 100x objective. Excitation was performed with a 532 nm cw laser (Laser Quantum, Opus). Excitation power was 0.5 mW and was kept constant for all measurements. Samples were placed face down on the inverted microscope and photoluminescence was measured by a photomultiplier after passing through a bandpass filters centred on the PL bands of the respective polymers.

3. RESULTS AND DISCUSSION

Figure 1 shows the electrical conductivity of PCPDTBT and P3HT thin films doped at different concentrations with F4-TCNQ.. The conductivity of both samples exhibits saturation after the initial increase of more than two orders of magnitude in conductivity. Conductivity for samples with doping between 0 and 5% shows a monotonous increase without a maximum (not shown). Interestingly, saturation occurs at different F4-TCNQ concentrations for the two polymers. In P3HT it saturates at 5% doping and decrease at high levels (>7.5%), whereas in PCPDTBT saturation occurs at 7.5%. For P3HT, a similar trend in conductivity has been recently reported by Duong et al.[19], although our saturation value for conductivity, 10^{-4} S/cm,

and saturation F4-TCNQ concentration are smaller than what other authors have reported ~10% [13]. We attribute this difference to the fact that the charge transport characteristics of P3HT depend dramatically on molecular weight [27]. In addition, our estimations of conductivity are performed with an impedance analysis that excludes displacement currents, injection resistance and ionic contributions which may result in larger values of the conductivity. Another important aspect of our experiments is that conductivity is measured at very low applied electric fields, which is a relevant variable for transport in organic semiconductors. In the following, we will discuss the correlation between the observation of dopant clustering and saturation in conductivity for both polymeric systems.

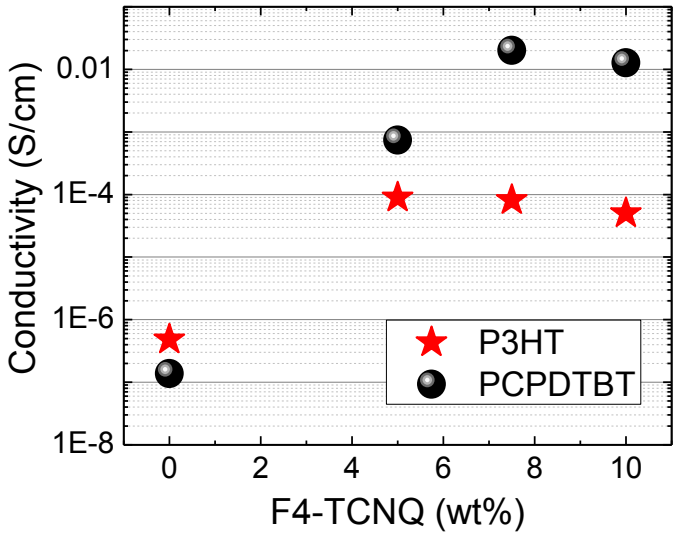

Figure 1. *Electrical conductivity of P3HT (red stars) and PCPDTBT (black dots) as a function of doping expressed as w/w% with respect to the polymer. Conductivity extracted from four probe experiments as detailed in the methods section.*

Figure 2(a-h) shows low-acceleration voltage (0.75 keV) SEM images of PCPDTBT thin films doped at different concentrations with F4-TCNQ. The films are deposited in the same manner as for the conductivity experiments, but on a highly doped silicon substrate with native oxide layer (few nm thick) and loaded in the SEM chamber without any further treatment. Throughout this paper we present our SEM data in two rows: in the *top row* we used the In-lens detector positioned within the electron column of the microscope, whereas in the *bottom row* a detector for SE2 placed to the side of the sample is used. The SE2 detector is expected to render mainly the surface morphological features, while the information provided by the In-lens detector should be more sensitive to material properties (atomic number contrast) and

electrostatic charging [28, 29]. Fig.2 (a and e) shows the pristine film surface morphology, exhibiting a fibrous texture with dimensions of the order of a few tens of nanometers. PCPDTBT is known to be a semi-crystalline polymer [30] and under the deposition conditions chosen here, we assign the fibres to domains with long range order. Interestingly, by doping 5% and 7.5% weight with respect to the polymer, Fig. 2(b-h), the original surface morphology of the pristine polymer seems to be slightly disrupted, i.e. the size of the fibres has substantially decreased. In addition, at 7.5% weight brighter regions appear, which are clearly apparent at 10% doping (Fig.2d and h) and grow further in area at doping >10% (not shown). Remarkably the In-lens image in Figure 2d shows a large contrast between what might be polymer rich domains (grey areas) and dopant rich domains (bright clusters) on the basis of relative concentration arguments and the experiments below. We point out that such contrast in SEM cannot be achieved in blends of PCPDTBT with other molecules with less pronounced electron affinities, such as the fullerene derivative PCBM (Fig S1 in supporting information), which are not capable of effectively doping the polymer in the ground state. Thus the observed contrast is unlikely to be caused by morphological effects due to blending with another molecule alone, but could arise from the electronic interaction connected to the doping process.

To further confirm the surface morphological changes we studied the same samples with a complementary technique which is sensitive only to the surface morphology. AFM images exhibit similar morphological patterns as observed in SEM (cf. Fig.S2 in supporting information). The high spatial resolution of the AFM technique is capable of clearly distinguishing the change in surface morphology induced by the dopant in going from 0% to 7.5%. On the basis of relative concentration arguments we raise here the hypothesis that the bright clusters in SEM can be assigned to dopant rich domains. In general, we can summarize the results on PCPDTBT doped with F4-TCNQ by reporting a change in the intrinsic morphology of the polymer when dopants are added at 5% concentration and, above 7.5%, formation of clusters with domains of about 200 nm in diameter, likely rich in dopant molecules.

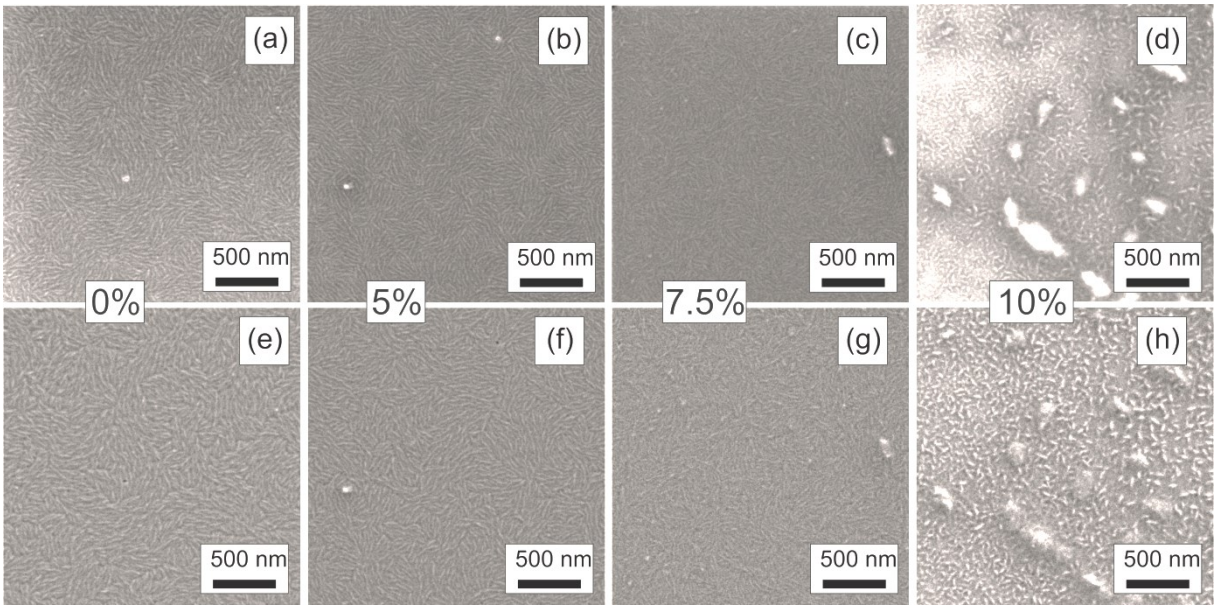

Figure 2. *Scanning electron microscopy images of PCPDTBT thin films doped with different amounts of F4-TCNQ, weight ratios are indicated in the respective figures. (a-d) images recorded with InLens and (e-h) SE2 detector.*

Figure 3(a-h) shows SEM images of P3HT doped with F4-TCNQ with identical weight ratios as those used for PCPDTBT. While the morphology of the pristine polymer appears less structured than the one of PCPDTBT, remarkably also for the P3HT samples there is an increase in image contrast which develops with increasing dopant concentration. However, in this case we observe a contrast at lower doping ratios (5%), than the doped PCPDTBT samples presented above. At 10% bright clusters are observed with diameters up to 500 nm, Fig.3d. The corresponding AFM images are shown in the supporting files (Fig. S3) where we note a corresponding change in the film morphology at 5% with the formation of clusters at 7.5 and 10% doping, in agreement with the morphological information obtained from the bottom row in Figure 3 (SE2 detector). We point out here that the overall grey-scale contrast of In-lens recorded images is slightly different in each picture, and cannot be equalized. This effect is physically related to the sample, as we discuss below. This is to explain that the apparent larger area of dopant rich domains in the 5% doped P3HT with respect to 10% is simply due to an inherently different contrast scale.

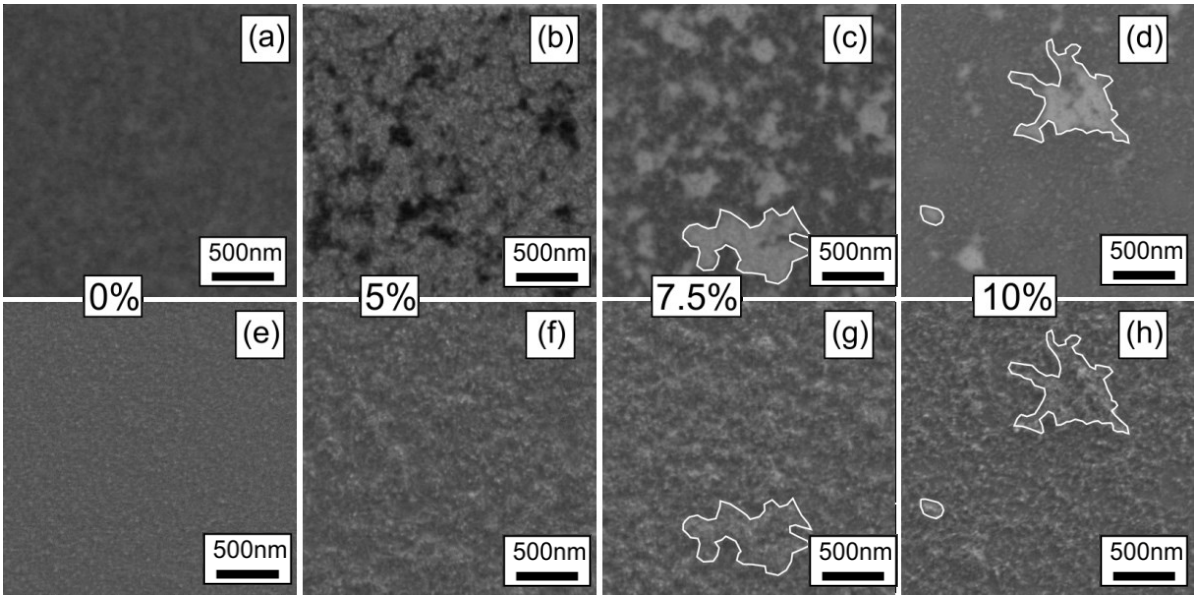

Figure 3. *Scanning electron microscopy images of P3HT thin films (doped with different amounts of F4-TCNQ, weight ratios are indicated in the respective figures. (a-d) images recorded with InLens and (e-h) SE2 detector. In panel c,d,g and h the regions with bright contrast have been marked to be clearly distinguished in the SE2 images.*

These results indicate that variations in the morphology of doped polymer films are correlated with changes in the electrical characteristics of doped samples as saturation in the electrical conductivity of the two polymers, at 5% for P3HT and 7.5% for PCPDTBT (Fig.1), occurs at dopant concentrations where clustering becomes apparent in SEM images. To confirm our assignment of the bright regions in the SEM images to dopant clusters we used confocal laser scanning microscopy. This technique can give unique insights on the morphology and thereby distinguish here between the electronic excited states of doped and pristine organic semiconductors [31-33]. A laser exciting the polymer photoluminescence (PL) is scanned over the sample and the PL is collected point by point, resulting in a 2D PL intensity map. Confocal microscopy is particularly suited to probe dopant distributions in our samples, since the extra charge carriers induced by the dopant molecules are known to quench PL of the host polymer via exciton-polaron quenching leaving dark areas in correspondence of dopant molecules [34, 35].

Figure 4(a-d) shows the PL imaging of the PCPDTBT films. We point out that confocal microscopy has a resolution comparable to the diffraction limit of the excitation light (~400 nm) therefore the fibres observed in the SEM and AFM images for the pristine PCPDTBT sample are not clearly distinguishable here. The most important aspect of these data is that upon

doping the overall PL intensity in the images decreases *homogeneously* in the whole field of view as shown in the inset images of Fig.4a-d. This behaviour is expected by comparing these PL results with the images of Fig.2. Due to the difference in resolution of confocal microscopy and SEM, dopant clusters smaller than 200 nm cannot be resolved here, and appear as homogenous darkening. Photogenerated excitons, which have a limited diffusion length, are quenched with high probability when dopants are distributed in many small clusters. This in turn leads to the observation of homogeneous and uniform PL quenching. In the case of P3HT, however, dopant rich domains reach diameters larger than the confocal microscope resolution and tend to phase segregate already at 5%, with lightly doped or undoped regions of several microns in between. These relatively large regions of the P3HT film which are unaffected or lightly doped are thus not subjected to severe exciton-polaron quenching and thus emit PL. Indeed, we observe that the doped P3HT films in Fig.5(e-h) show modulations in the PL intensity on a length scale of a micron and are consistent with the interpretation that the bright clusters of similar size seen in SEM are likely to be F4-TCNQ rich areas.

As we show from Monte-Carlo simulations in supporting material (Fig. S4-S5), our SEM experiments are sensitive to the surface morphology within the first 15 nm of the film. It is thus important to clarify if the separation of F4-TCNQ rich and poor domains, visible in the SEM, is present throughout the bulk of the film. To address this important question, we performed TEM on samples prepared in the same conditions and delaminated from the silicon substrate. Figure 5 shows TEM images of the different samples. While the surface morphological features, observed in SEM with the SE2 detector are difficult to distinguish here, a larger contrast between different domains is present in the doped samples. Because of the transmission detection geometry, darker areas are ascribed to regions with high electron scattering probability and thus rich in F4-TCNQ, analogous to the contrast observed in polymer:fullerene blends [36, 37]. We notice that at 5% doping P3HT displays clusters rich in dopant molecules and the information obtained from SEM is thereby confirmed (Fig.5f). For PCPDTBT (Fig.5b) we notice small clusters with dimensions below 100 nm, which are not observable in SEM. On the other hand when clusters reach dimensions of the order of hundreds of nanometers (Fig.5c and d), such as at 7.5%, they may be observable in SEM, since their size is comparable to or even larger than the film thickness.

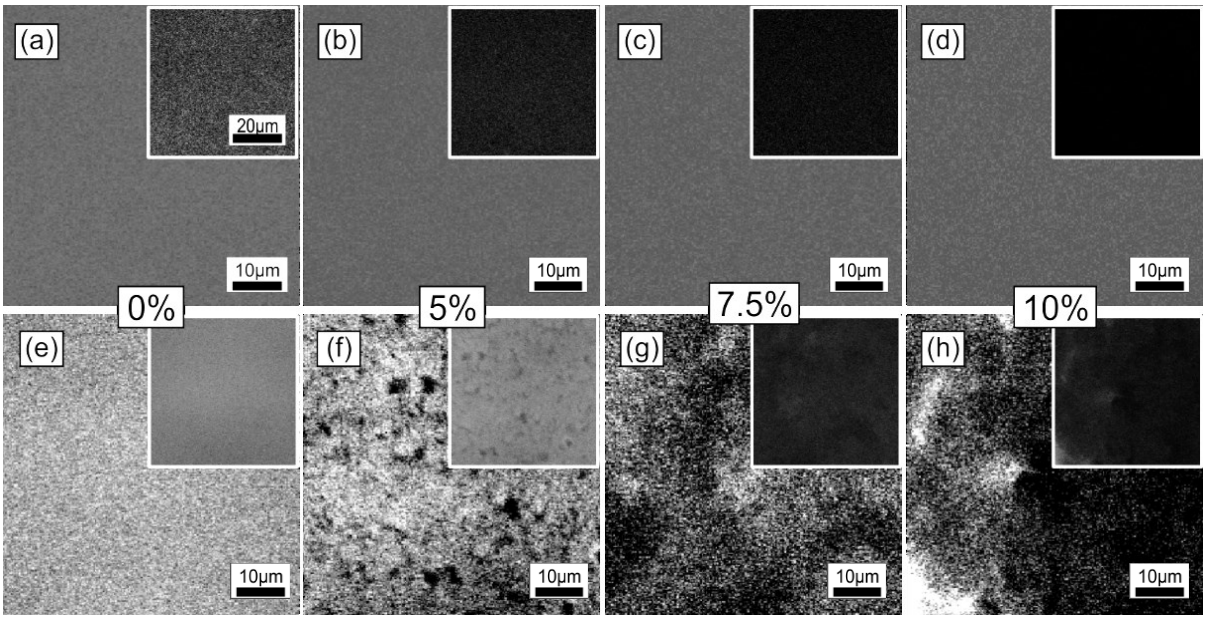

Figure 4. *Photoluminescence images for PCPDTBT (a-d) and P3HT (e-h) thin films doped with F4-TCNQ at different ratios as indicated in the figure. Images were post-processed for optimal contrast, the insets show the unprocessed images on a common PL intensity scale and same image size. Excitation wavelength is 532 nm.*

The SEM images presented in Fig.2 and Fig.3 indicate how low-voltage SEM is a powerful technique to map the in plane distribution of dopants and surface morphology in a polymeric semiconductor thin film. It has been shown in previous publications [38, 39] that because of the small dielectric constant of these materials, the electrostatic interactions between the ionized dopant and the polymer molecules can be substantial. This may create spatial variations in the electric potential which perturbs the normal assembly of pristine polymer chains in the solid state. Another aspect suggested by our experiments is that F4-TCNQ molecules have the tendency to aggregate or form clusters above a critical dopant concentration. This critical concentration may be influenced by the properties of the polymer. The minimum amount of dopant that can be introduced in the polymer film without altering the film surface morphology in an appreciable way is larger for PCPDTBT than for P3HT. One possible explanation for this is that the donor-acceptor structure of PCPDTBT, which has intrinsic on-chain dipoles,[25, 40] is capable of screening the interaction between the ionized dopants and ionized segments of the polymer chain. This could help avoiding clustering already in the starting solution before the deposition process.

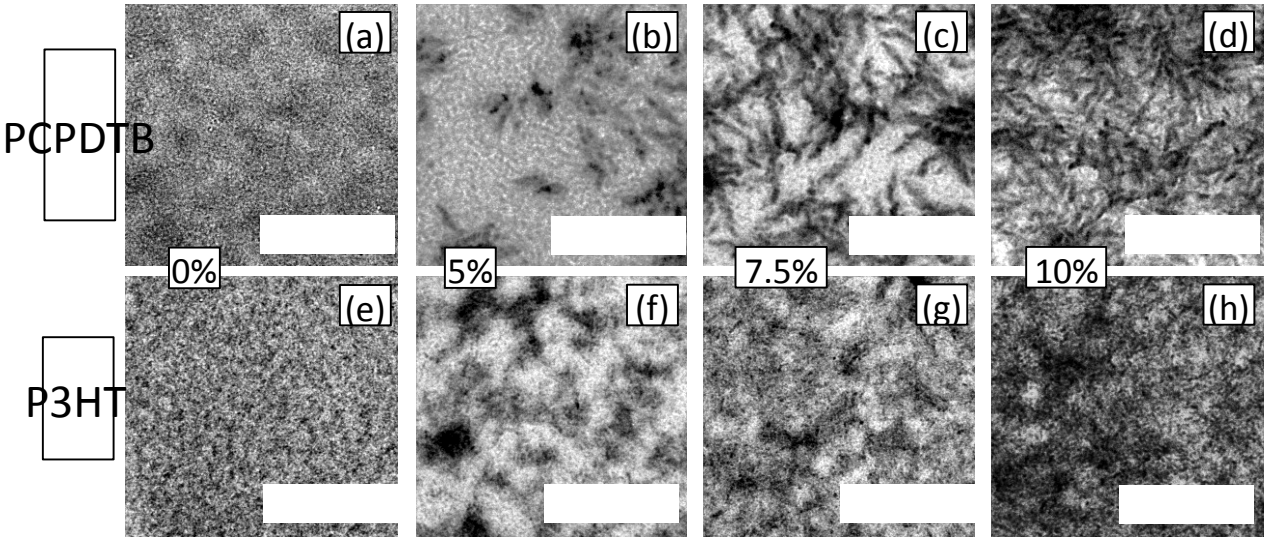

Figure 5. *TEM images for PCPDTBT (a-d) and P3HT (e-h) thin films doped with F4-TCNQ at different ratios as indicated in the figure. Acceleration voltage 100 kV*.

One possible reason for the observed contrast difference might be a local increase in the film thickness at the cluster sites rich in dopant, which corresponds to an increased roughness (AFM measurements - Fig.S2 and Fig.S4). This effect, however, can be ruled out due to the small (ca. 15 nm) penetration depth of the electron beam in the organic materials at the applied acceleration voltage of 0.75 keV as we demonstrate in our Monte-Carlo simulations (Fig. S4). This penetration depth is much smaller than the average film thickness of the samples (~100 nm) and also changes in roughness unlikely result in such a defined contrast with the In-lens detector. Another possible explanation for the contrast could be the difference in atomic numbers between the polymer and the dopants, since the electron backscattering process involves the interaction between the accelerated electrons and the nuclei of the investigated materials [29]. However, the difference between the mean atomic numbers of the nuclei in the organic molecules used here is generally very small, resulting in only a marginal difference in the backscattered electron yields, when calculated using our simulations (Supporting material Fig.S5). Also the low atomic numbers of these materials suggest that the contribution of backscattered electrons in the image formation, either using the In-lens or SE2 detector, should be minor compared to the scattered electrons emerging due to *inelastic* scattering processes and thus clearly excludes a material or *chemical* contrast.

Interestingly while recording the SEM images we observed that the contrast evolves during acquisition and can be related to the exposure time of the doped samples to the electron

beam. In contrast to doped samples, when a pure polymer film is investigated, it becomes gradually darker with exposure time in a rather homogenous manner (Fig. S6a). This is indicative of a charge build-up or a lower yield in electron emerging from the sample surface [41]. The contrast development in doped films is reported in Fig. S6b of the supplementary material and is most probably due to a different charging behaviour of the dopant rich domains. By measuring the time until a full "exposure" of the film, i.e. no further change in contrast is observed, we can calculate the necessary electron beam density for full development to be 1.6×10^9 μm^{-2}. It is an interesting question how this value compares to the number of dopant molecules. The area density of F4-TCNQ molecules can be calculated using the density of P3HT [42] (1.1 g/cm³) and F4-TCNQ [43] (1.4 g/cm³) together with the film thickness of 100 nm. We obtain a dopant area density of 1.2×10^5 μm^{-2} for a doping ratio of 5%. The number of dopant molecules is lower than the number of electrons per area needed for full exposure of the film. We would ideally expect that one electron per dopant molecule is necessary for contrast development. This difference points to the fact that not all dopants are homogeneously dispersed and probably also not all ionized in the film. The film regions with undoped polymer appear to be more affected by charging rather than the doped areas.

The gradual darkening of a pure polymer film indicates that the darker regions in the fully exposed SEM images of doped films are more similar to the pure polymer, i.e. dopant deficient. At the same time F4-TCNQ is expected to be negatively charged while the doped polymer in close proximity positively charged, thus capable of accepting electrons from the scanning beam. We assign the positive contrast of the F4-TCNQ rich domains in the film to *electron accumulation* in the doped regions and thus enhanced scattering by Coulomb repulsion of the incoming electrons after several scans. This effect results in a significantly increased number of electrons backscattered and collected by the detector, giving rise to the contrast enhancement in the In-lens image. We note that the electron dose necessary to develop a contrast stated above, corresponding to $2.56\ 10^{-2}$ C/cm^2, is in remarkably good agreement with values of the critical charging dose for most organic compounds studied by low voltage electron microscopy [44, 45]. On the basis of our experiments alone we cannot provide any quantitative statement on the amount of charged and neutral F4-TCNQ molecules in clusters. Ideally this would require a near field scanning probe technique sensitive to conductivity such as conductive AFM [20] or more sophisticated approaches such as Auger photoelectron spectroscopy mapping, which are not available to us.

In correlating this electron microscopy study with the results of the electrical characterization reported in Fig.1 we stress that saturation in the values of conductivity seem to

be linked to the appearance of clusters rich in dopant molecules. To base our discussion on a more quantitative analysis of the images, we have measured the perimeter of several clusters as detailed in the method section. P3HT exhibits saturation in conductivity at 5% dopant ratio, where clusters with an average perimeter size larger than 500 nm are the 13% of all the clusters detected by SEM. This indicates that F4-TCNQ molecules in cluster are less likely capable of acting as electron acceptors and to effectively dope the P3HT conjugated segments. The shift in the saturation conductivity for PCPDTBT at 7.5% doping ratio is reflected in a significant clustering occurring mainly at this ratio or higher. For PCPDBT, we were able to provide a quantitative estimation of the cluster perimeter size only for the 10% sample (see Fig.S7), where clusters with an average perimeter of 500 nm are 22% of all the cluster detected. As a comparison the 10% doped P3HT sample has 31% of all clusters with an average perimeter larger than 500 nm. These quantitative estimations on morphological aspects provide also valid arguments to discuss the higher absolute conductivity of doped PCPDTBT with respect to P3HT.

4. CONCLUSIONS

We used the strong electron acceptor F4-TCNQ to dope P3HT and the copolymer PCPDTBT. Low voltage SEM is employed to monitor the surface morphology of polymeric semiconductor thin films and in parallel to characterize the distribution of dopants at the nanometer scale. We show that the polymer/dopant blends undergo phase separation above certain dopant concentrations, resulting in a significant morphology change of the films which can be correlated with saturation in the conductivity of the materials. These critical concentration values depend on the structural and chemical properties of the conjugated polymer. Our results have implications for the field of doped organic semiconducting devices and demonstrate how SEM can be used as a fast technique for screening dopant distributions and helping the understanding of relationships between electrical properties and morphology in conjugated polymer systems.

Supporting Information

AFM of all samples, Monte Carlo simulations of electron scattering yield, time evolution of SEM images and image statistical analysis.

Corresponding Author
*Email: edc25@bath.ac.uk. Tel: +44-1225-384368, Fax: +44-1225-386110

Notes

[±] present address: Optoelectronics Group, Cavendish Laboratory, University of Cambridge, Cambridge (U.K.)

[ǂ] present address: AlphaLaser GmbH Munich (Germany)

[÷] present address: SiCrystal AG, Nurnberg (Germany)

Acknowledgements

We thank S. Niedermaier and A. Helfrich for technical assistance. We are grateful to the DFG for financial support through the SPP1355 "Fundamental processes in organic photovoltaics" " and the Bavarian State Ministry of Science, Research, and the Arts through the Collaborative Research Network ''Solar Technologies go Hybrid''. The German Excellence Initiative is also acknowledged for funding via the "Nanosystems Initiative Munich (NIM)" and the LMUexcellent Research Fellowship.

References

[1] C. Falkenberg, C. Uhrich, S. Olthof, B. Maennig, M.K. Riede, K. Leo, Efficient p-i-n type organic solar cells incorporating 1,4,5,8-naphthalenetetracarboxylic dianhydride as transparent electron transport material, J. Appl. Phys., 104 (2008) 034506.

[2] S. Reineke, F. Lindner, G. Schwartz, N. Seidler, K. Walzer, B. Lussem, K. Leo, White organic light-emitting diodes with fluorescent tube efficiency, Nature, 459 (2009) 234-238.

[3] A. Tunc, A. De Sio, D. Riedel, F. Deschler, E. Da Como, J. Parisi, E. Von Hauff, Org. Elect., 13 (2012) 290-296.

[4] A. Loiudice, A. Rizzo, M. Biasiucci, G. Gigli, Bulk Heterojunction versus Diffused Bilayer: The Role of Device Geometry in Solution p-Doped Polymer-Based Solar Cells, J. Phys. Chem. Lett., 3 (2012) 1908-1915.

[5] C.K. Chan, W. Zhao, A. Kahn, I.G. Hill, Influence of chemical doping on the performance of organic photovoltaic cells, Appl. Phys. Lett., 94 (2009) 203306.

[6] H. Li, P. Winget, J.L. Bredas, Surface Modification of Indium-Tin-Oxide Via Self-Assembly of a Donor-Acceptor Complex: A Density Functional Theory Study, Adv. Mater., 24 (2012) 687-693.

[7] E.L. Hanson, J. Guo, N. Koch, J. Schwartz, S.L. Bernasek, Advanced surface modification of indium tin oxide for improved charge injection in organic devices, J. Am. Chem. Soc., 127 (2005) 10058-10062.

[8] Y.A. Zhang, P.W.M. Blom, Enhancement of the hole injection into regioregular poly(3-hexylthiophene) by molecular doping, Appl. Phys. Lett., 97 (2010) 083303.

[9] K. Harada, M. Riede, K. Leo, O.R. Hild, C.M. Elliott, Pentacene homojunctions: Electron and hole transport properties and related photovoltaic responses, Phys. Rev. B, 77 (2008) 195212.

[10] S. Olthof, S. Mehraeen, S.K. Mohapatra, S. Barlow, V. Coropceanu, J.L. Bredas, S.R. Marder, A. Kahn, Ultralow Doping in Organic Semiconductors: Evidence of Trap Filling, Phys. Rev. Lett., 109 (2012) 176601.

[11] Y.Y. Lai, P.I. Shih, Y.P. Li, C.E. Tsai, J.S. Wu, Y.J. Cheng, C.S. Hsu, Interface Engineering to Enhance the Efficiency of Conventional Polymer Solar Cells by Alcohol-/Water-Soluble C-60 Materials Doped with Alkali Carbonates, ACS Appl. Mater. Interfaces, 5 (2013) 5122-5128.

[12] F. Deschler, E. Da Como, T. Limmer, R. Tautz, T. Godde, M. Bayer, E. von Hauff, S. Yilmaz, S. Allard, U. Scherf, J. Feldmann, Reduced charge transfer exciton recombination in organic semiconductor heterojunctions by molecular doping, Phys. Rev. Lett., 107 (2011) 127402.

[13] K.H. Yim, G.L. Whiting, C.E. Murphy, J.J.M. Halls, J.H. Burroughes, R.H. Friend, J.S. Kim, Controlling electrical properties of conjugated polymers via a solution-based p-type doping, Adv. Mater., 20 (2008) 3319-3324.

[14] M.C. Gwinner, R. Di Pietro, Y. Vaynzof, K.J. Greenberg, P.K.H. Ho, R.H. Friend, H. Sirringhaus, Doping of Organic Semiconductors Using Molybdenum Trioxide: a Quantitative Time-Dependent Electrical and Spectroscopic Study, Adv. Funct. Mater., 21 (2011) 1432-1441.

[15] S.D. Ha, A. Kahn, Isolated molecular dopants in pentacene observed by scanning tunneling microscopy, Phys. Rev. B, 80 (2009) 195410.

[16] P. Pingel, L.Y. Zhu, K.S. Park, J.O. Vogel, S. Janietz, E.G. Kim, J.P. Rabe, J.L. Bredas, N. Koch, Charge-Transfer Localization in Molecularly Doped Thiophene-Based Donor Polymers, J. Phys. Chem. Lett., 1 (2010) 2037-2041.

[17] E.F. Aziz, A. Vollmer, S. Eisebitt, W. Eberhardt, P. Pingel, D. Neher, N. Koch, Localized charge transfer in a molecularly doped conducting polymer, Adv. Mater., 19 (2007) 3257-3260.

[18] H. Kleemann, C. Schuenemann, A.A. Zakhidov, M. Riede, B. Lussem, K. Leo, Structural phase transition in pentacene caused by molecular doping and its effect on charge carrier mobility, Org. Elect., 13 (2012) 58-65.

[19] D.T. Duong, C.C. Wang, E. Antono, M.F. Toney, A. Salleo, The chemical and structural origin of efficient p-type doping in P3HT, Org. Elect., 14 (2013) 1330-1336.

[20] D.T. Duong, H. Phan, D. Hanifi, P. Sung Jo, T.Q. Nguyen, A. Salleo, Direct Observation of Doping Sites in Temperature-Controlled, p-Doped P3HT Thin Films by Conducting Atomic Force Microscopy, Adv. Mater., 26 (2014) 6069-6073.

[21] A. Salleo, R.J. Kline, D.M. DeLongchamp, M.L. Chabinyc, Microstructural Characterization and Charge Transport in Thin Films of Conjugated Polymers, Adv. Mater., 22 (2010) 3812-3838.

[22] H. Hoppe, M. Niggemann, C. Winder, J. Kraut, R. Hiesgen, A. Hinsch, D. Meissner, N.S. Sariciftci, Nanoscale morphology of conjugated polymer/fullerene-based bulk-heterojunction solar cells, Adv. Funct. Mater., 14 (2004) 1005-1011.

[23] O.D. Paraschuk, S. Grigorian, E.E. Levin, V.V. Bruevich, K. Bukunov, I.V. Golovnin, T. Dittrich, K.A. Dembo, V.V. Volkov, D.Y. Paraschuk, Acceptor-Enhanced Local Order in Conjugated Polymer Films, J. Phys. Chem. Lett., 4 (2013) 1298-1303.

[24] D. Donhauser, M. Pfannmoeller, L. Dieterle, K. Schultheiss, R.R. Schroeder, W. Kowalsky, M. Kroeger, Adv. Funct. Mater., 23 (2013) 2130-2136.

[25] R. Tautz, E. Da Como, T. Limmer, J. Feldmann, H.-J. Egelhaaf, E. von Hauff, V. Lemaur, D. Beljonne, S. Yilmaz, I. Dumsch, S. Allard, U. Scherf, Structural correlations in the generation of polaron pairs in low-bandgap polymers for photovoltaics, Nat Commun, 3 (2012) 970.

[26] R. Tautz, E. Da Como, C. Wiebeler, G. Soavi, I. Dumsch, N. Frohlich, G. Grancini, S. Allard, U. Scherf, G. Cerullo, S. Schumacher, J. Feldmann, Charge Photogeneration in Donor-Acceptor Conjugated Materials: Influence of Excess Excitation Energy and Chain Length, J. Am. Chem. Soc., 135 (2013) 4282-4290.

[27] R. Noriega, J. Rivnay, K. Vandewal, F.P.V. Koch, N. Stingelin, P. Smith, M.F. Toney, A. Salleo, A general relationship between disorder, aggregation and charge transport in conjugated polymers, Nature Mater., 12 (2013) 1037-1043.

[28] L. Reimer, Scanning Electron Microscopy, Springer-Verlag, Berlin, 1998.

[29] R.F. Egerton, Physical Principles of Electron Microscopy Springer, New York, 2005.

[30] M. Morana, M. Wegscheider, A. Bonanni, N. Kopidakis, S. Shaheen, M. Scharber, Z. Zhu, D. Waller, R. Gaudiana, C. Brabec, Bipolar charge transport in PCPDTBT-PCBM bulk-heterojunctions for photovoltaic applications, Adv. Funct. Mater., 18 (2008) 1757-1766.

[31] E. Da Como, M.A. Loi, M. Murgia, R. Zamboni, M. Muccini, J-aggregation in alpha-sexithiophene submonolayer films on silicon dioxide, J. Am. Chem. Soc., 128 (2006) 4277-4281.

[32] M.A. Loi, E. Da Como, F. Dinelli, M. Murgia, R. Zamboni, F. Biscarini, M. Muccini, Supramolecular organization in ultra-thin films of alpha-sexithiophene on silicon dioxide, Nature Mater., 4 (2005) 81-85.

[33] A.W. Tsen, F. Cicoira, G.G. Malliaras, J. Park, Photoelectrical imaging and characterization of point contacts in pentacene thin-film transistors, Appl. Phys. Lett., 97 (2010) 023308.

[34] J.C. Bolinger, M.C. Traub, T. Adachi, P.F. Barbara, Ultralong-Range Polaron-Induced Quenching of Excitons in Isolated Conjugated Polymers, Science, 331 (2011) 565-567.

[35] S. Reineke, K. Walzer, K. Leo, Triplet-exciton quenching in organic phosphorescent light-emitting diodes with Ir-based emitters, Phys. Rev. B, 75 (2007) 125328.

[36] S.S. van Bavel, M. Barenklau, G. de With, H. Hoppe, J. Loos, P3HT/PCBM Bulk Heterojunction Solar Cells: Impact of Blend Composition and 3D Morphology on Device Performance, Adv. Funct. Mater., 20 (2010) 1458-1463.

[37] M. Hallermann, E. Da Como, J. Feldmann, M. Izquierdo, S. Filippone, N. Martin, S. Juchter, E. von Hauff, Correlation between charge transfer exciton recombination and photocurrent in polymer/fullerene solar cells, Appl. Phys. Lett., 97 (2010) 023301.

[38] Y. Zhang, B. de Boer, P.W.M. Blom, Trap-free electron transport in poly(p-phenylene vinylene) by deactivation of traps with n-type doping, Phys. Rev. B, 81 (2010) 085201.

[39] Y. Zhang, B. de Boer, P.W.M. Blom, Controllable Molecular Doping and Charge Transport in Solution-Processed Polymer Semiconducting Layers, Adv. Funct. Mater., 19 (2009) 1901-1905.

[40] B. Carsten, J.M. Szarko, H.J. Son, W. Wang, L.Y. Lu, F. He, B.S. Rolczynski, S.J. Lou, L.X. Chen, L.P. Yu, Examining the effect of the dipole moment on charge separation in donor-acceptor polymers for organic photovoltaic applications, J. Am. Chem. Soc., 133 (2011) 20468-20475.

[41] R.F. Egerton, P. Li, M. Malac, Radiation damage in the TEM and SEM, Micron, 35 (2004) 399-409.

[42] T.J. Prosa, M.J. Winokur, J. Moulton, P. Smith, A.J. Heeger, X-RAY STRUCTURAL STUDIES OF POLY(3-ALKYLTHIOPHENES) - AN EXAMPLE OF AN INVERSE COMB, Macromolecules, 25 (1992) 4364-4372.

[43] W.Y. Gao, A. Kahn, Electronic structure and current injection in zinc phthalocyanine doped with tetrafluorotetracyanoquinodimethane: Interface versus bulk effects, Org. Elect., 3 (2002) 53-63.

[44] L.F. Drummy, J.Y. Yang, D.C. Martin, Low-voltage electron microscopy of polymer and organic molecular thin films, Ultramicroscopy, 99 (2004) 247-256.

[45] M.R. Stevens, Q. Chen, U. Weierstall, J.C.H. Spence, Transmission electron diffraction at 200 eV and damage thresholds below the carbon K edge, Microsc. microanal., 6 (2000) 368-379.